HHS Public Access

Author manuscript

Chemphyschem. Author manuscript; available in PMC 2019 October 19.

Published in final edited form as:

Chemphyschem. 2018 October 19; 19(20): 2621–2626. doi:10.1002/cphc.201800690.

Heterogeneous Parahydrogen Pairwise Addition to Cyclopropane

Oleg G. Salnikov[a,b], **Kirill V. Kovtunov**[a,b] **[Dr.]**, **Panayiotis Nikolaou**[c] **[Dr.]**, **Larisa M. Kovtunova**[d,b] **[Dr.]**, **Valerii I. Bukhtiyarov**[d,b] **[Prof.]**, **Igor V. Koptyug**[a,b] **[Prof.]**, and **Eduard Y. Chekmenev**[c,e,f] **[Prof.]**

[a]International Tomography Center, SB RAS, 3A Institutskaya st., Novosibirsk 630090, Russia, salnikov@tomo.nsc.ru

[b]Novosibirsk State University, 2 Pirogova st., Novosibirsk 630090, Russia

[c]Vanderbilt University Institute of Imaging Science (VUIIS), Department of Radiology, Department of Biomedical Engineering, and Vanderbilt-Ingram Cancer Center (VICC), Vanderbilt University Medical Center, Nashville, TN 37232-2310, United States

[d]Boreskov Institute of Catalysis, SB RAS, 5 Acad. Lavrentiev pr., Novosibirsk 630090, Russia

[e]Russian Academy of Sciences, 14 Leninskiy prospect, Moscow 119991, Russia

[f]Department of Chemistry, Integrative Biosciences (Ibio), Wayne State University, Karmanos Cancer Institute (KCI), Detroit, MI 48202, United States, chekmenev@wayne.edu

Abstract

Hyperpolarized gases revolutionize functional pulmonary imaging. Hyperpolarized propane is a promising emerging contrast agent for pulmonary MRI. Unlike hyperpolarized noble gases, proton-hyperpolarized propane gas can be imaged using conventional MRI scanners with proton imaging capability. Moreover, it is non-toxic odorless anesthetic. Furthermore, propane hyperpolarization can be accomplished by pairwise addition of parahydrogen to propylene. Here, we demonstrate the feasibility of propane hyperpolarization via hydrogenation of cyclopropane with parahydrogen. ^{1}H propane polarization up to 2.4% is demonstrated here using 82% parahydrogen enrichment and heterogeneous Rh/TiO_2 hydrogenation catalyst. This level of polarization is several times greater than that of propylene precursor under the same conditions despite the fact that direct pairwise addition of parahydrogen to cyclopropane may also lead to formation of propane with NMR-invisible hyperpolarization due to magnetic equivalence of nascent parahydrogen protons in two CH_3 groups. NMR-visible hyperpolarized propane demonstrated here can be formed only via a reaction pathway involving cleavage of at least one C–H bond in the reactant molecule. The resulting NMR signal enhancement of hyperpolarized propane was sufficient for 2D gradient echo MRI of ~5.5 mL phantom with 1×1 mm^2 spatial resolution and 64×64 imaging matrix despite relatively low chemical conversion of cyclopropane substrate.

Correspondence to: Oleg G. Salnikov; Eduard Y. Chekmenev.

Supporting information for this article is given via a link at the end of the document.

Entry for the Table of Contents

Layout 1:

COMMUNICATION

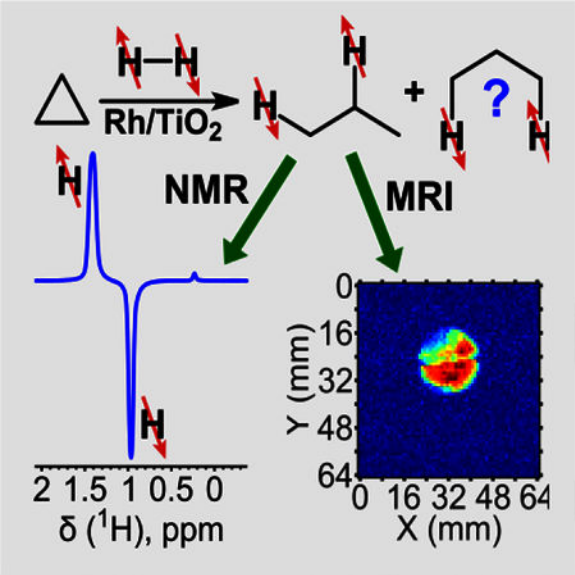

Heterogeneous hydrogenation of cyclopropane with parahydrogen over Rh/TiO_2 catalyst was shown to be a promising approach for production of propane gas with high level of proton polarization suitable for magnetic resonance imaging applications.

Keywords

hyperpolarization; parahydrogen-induced polarization; cyclopropane; contrast agent; hydrogenation

---

Despite its high importance as a powerful tool for clinical diagnostics of various diseases and pathologies, magnetic resonance imaging (MRI) suffers from inherently low sensitivity caused by low (10^{-6}-10^{-5}) nuclear spin polarization *P*. The low sensitivity issue additionally exacerbates the challenges for MRI of lungs due to their inherently low spin density. As a result, computed tomography (CT) and chest radiography are typically used for clinical pulmonary imaging of chronic obstructive pulmonary disease (COPD).[1, 2] However, these techniques have drawbacks of (i) a patient exposure to ionizing radiation, and (ii) lacking functional information to report on gas ventilation, diffusion and perfusion.

Hyperpolarization of nuclear spins is a highly efficient way to boost the sensitivity of NMR and MRI through the increase of *P* by several orders of magnitude.[1–3] Hyperpolarization techniques such as dynamic nuclear polarization (DNP),[4–7] spin-exchange optical pumping (SEOP) of noble gases,[1, 2, 8–10] and parahydrogen-induced polarization (PHIP)[11–15] can produce hyperpolarized (HP) gases, which can be potentially inhaled. The inhaled HP gas can be imaged on a single breath hold resulting in 2D and 3D functional MRI images of gas ventilation, diffusion and perfusion.[2, 16, 17] Currently, the most widely used HP gases are

^{129}Xe and ^{3}He, produced by SEOP[1, 2, 18] and successfully utilized for preclinical and clinical imaging of COPD.[2, 19–23] However, SEOP requires sophisticated hyperpolarization hardware (including high-power lasers), and has a throughput limitation of a few liters of HP gas per hour.[24–31] Moreover, HP noble gases (^{3}He, ^{129}Xe, etc.) cannot be directly imaged on clinical MRI scanners, because they require heteronuclear MRI hardware and software capabilities, which is currently available only on highly-specialized research MRI scanners. PHIP is a significantly less expensive and faster alternative to SEOP. PHIP has been shown to produce proton-HP gases, e.g. propane,[32–36] which can be detected on any conventional MRI scanner. PHIP is based on a pairwise addition of two atoms from the same parahydrogen (p-H_2) molecule to an asymmetric unsaturated substrate molecule[11, 12] over homogeneous[37] or heterogeneous[38] hydrogenation catalyst.

Recent progress in heterogeneous catalytic systems[32, 38–40] has achieved more than 10% contribution of pairwise p-H_2 addition (i.e. polarization P_H exceeding 10%).[41, 42] Moreover, heterogeneous catalysts are robust and well-suited for production of pure from catalyst HP gases for potential *in vivo* and clinical use for pulmonary and other bioimaging applications. Currently, one of the most promising proton-HP candidates for *in vivo* applications is propane gas.[1, 43–45] Propane has low toxicity since it is not readily absorbed and is not biologically active, and can be administered *in vivo* via inhalation as an anesthetic.[46] HP propane can be produced by pairwise addition of p-H_2 to propylene over a number of heterogeneous catalysts.[32] However, the use of propylene is undesirable in case of its incomplete conversion because of propylene unpleasant odor.

In this communication, we explore the feasibility of production of HP propane gas via hydrogenation of cyclopropane with p-H_2. The advantage of cyclopropane as an unsaturated precursor for HP propane production is its well-established prior use in anesthesia.[47] Since cyclopropane does not contain C=C bonds, it is unlikely that it could be coordinated to a transition metal complex and, hence, hydrogenated over this type of catalyst. Indeed, no reaction was observed between cyclopropane and p-H_2 in the presence of homogeneous catalyst [Rh(NBD)(dppb)]BF_4 in CD_3OD (NBD = norbornadiene, dppb = 1,4-bis(diphenylphosphino)butane), i.e. under conditions when highly polarized propane is formed from propylene and p-H_2 mixture.[48]

In principle, considering the broad range of processes which may occur on the surface of supported metal nanoparticles during hydrogenation,[49–52] the reaction of cyclopropane with p-H_2 over supported metal catalysts may lead to three types of HP propane molecules with p-H_2-derived protons in CH_3 group and CH_2 group via route #1, in two different CH_3 groups via route #2 or in the same CH_3 group via route #3 (Scheme 1a). The routes #2 and #3 are of particular interest, because pH_2-derived protons are located in magnetically equivalent positions in reaction product molecules. Due to magnetic equivalence, hyperpolarization of these molecules cannot be revealed by direct NMR spectroscopy, similarly to singlet state of p-H_2 molecule or nuclear spin isomers of ethylene produced by pairwise addition of p-H_2 to acetylene.[53] NMR spectra simulations of such spin states of HP propane performed using standard density matrix formalism indeed show that no NMR signal should occur from p-H_2 derived protons. On the other hand, these symmetric states of

HP propane could be very long lived similar to p-H_2 and nuclear spin isomers of ethylene, [53] making them potentially possible to use as a reservoir for storage of hyperpolarization.

The performance of three supported metal catalysts (Pt/TiO_2, Pd/TiO_2 and Rh/TiO_2) in cyclopropane hydrogenation was studied in PASADENA[12] conditions, i.e. when hydrogenation with p-H_2 was carried out in high magnetic field of NMR spectrometer inside a 5 mm NMR tube. Pd/TiO_2 catalyst did not show considerable activity in flow conditions though slow formation of propane was observed after interruption of gas flow (Figure 1c). Pt/TiO_2 catalyst was the most active; indeed, propane was formed even at flow conditions but PHIP effects were not detected (Figure 1b). In contrast, utilization of Rh/TiO_2 catalyst allowed to observe pronounced PASADENA signals of HP propane in flow conditions (Figure 1a) similar to those observed in PASADENA hydrogenation of propylene.[38] This result is consistent with several previous studies on hydrogenation of alkenes with p-H_2, where it was shown that $RhTiO_2$ catalyst provides higher PHIP signals intensities than Pt/TiO_2 or Pd/TiO_2, indicating that contribution of route of pairwise H_2 addition to C=C bonds is greater in the case of Rh/TiO_2.[32, 52] The estimated polarizations of HP propane produced from hydrogenation of cyclopropane on Rh/TiO_2 were $\%P_H$~0.34–0.84% at 82% p-H_2 enrichment depending on reactants' gas flow rates. These values are the lower estimates of propane polarizations, because spectra acquired after interruption of gas flow and complete relaxation of HP state were used as thermal references. Therefore, some additional amount of reaction product may be formed during this delay leading to overestimation of the denominator of P_H calculation. At the same time, overall hydrogenation activity of Rh catalyst in PASADENA conditions was very low (≤1% conversion of cyclopropane). Rh/TiO_2 catalyst was also tested in liquid phase hydrogenation of cyclopropane with p-H_2 in CD_3OD and yielded some weak PASADENA signals of HP propane (Figure S1).

Due to relatively low efficiency of PASADENA hydrogenation of cyclopropane, we explored the possibility of performing hydrogenation reaction outside the NMR spectrometer in the Earth's magnetic field (ALTADENA[54] conditions) using a high-pressure setup with temperature control. In our case, the maximum signals were observed at 720 standard cubic centimetres per minute (sccm) total gas flow rate (Figure S2). Conversion values at these conditions did not exceed 0.3%, despite the use of higher catalyst loads (Table S1). Temperature dependence indicates that moderate temperature (~110–135 °C) is needed in order to obtain the most intensive ALTADENA signals (Figure S3). Despite the low reaction yield, the use of cyclopropane as a precursor of HP propane is promising due to remarkably high levels of polarization. The highest obtained signal enhancement was 460–480, corresponding to 1.5–1.6% ^1H polarization (Table S1). The polarization levels obtained using propylene as a precursor were ~4 times lower under conditions of optimized temperature and otherwise similar experimental parameters at nearly 100% conversion.

To explore the possibility of the use of HP propane (produced from cyclopropane) for MRI, the reactor containing >2 times Rh/TiO_2 catalyst load (280 mg vs. 118 mg) was prepared. First, the resultant setup was tested in ALTADENA conditions. The increased catalyst loading allowed to reach 2.8% cyclopropane conversion with SE = 600–620, corresponding

to 1.9–2.0% propane polarization (Figure 2). Notably, both chemical conversion and P_H were enhanced with this catalyst load compared to the previous load under otherwise similar conditions. Higher propane polarization was observed (SE = 740–750, 2.4% propane polarization) at doubled gas flow rates (likely due to reduced %P_H relaxation), though at the expense of cyclopropane conversion (0.7%). The polarization levels of obtained HP propane were indeed sufficient for MRI (despite very low conversion levels), as was demonstrated on the example of 2D gradient echo (GRE) MRI of a ~5.5 mL phantom, acquired with 1×1 mm^2 spatial resolution and 64×64 imaging matrix (Figure 3). Importantly, these images are the first demonstration of high field MRI of HP propane in a stopped flow mode, contrary to previously shown high field MRI of continuously flowing HP propane gas.[32] The feasibility of stopped flow MRI is important, because this regime will be implemented in case of HP propane inhalation by a patient. Considering relatively fast T_1 relaxation of HP propane, the possibility to obtain its MR image a few seconds after interruption of gas flow demonstrates the promising prospects for application of HP propane as a contrast agent for lung MRI.

The observation of such high levels of propane polarization in cyclopropane hydrogenation is unexpected, because only route #1 (see Scheme 1a) contributes to the observable PHIP signal, while all propane molecules prepared via routes #1–3 as well as via non-pairwise hydrogen addition contribute to the signal of thermally polarized propane used as a reference for SE and %P_H estimation. Moreover, intuitively route #2 should be preferred over route #1 for ring opening, since the former is most likely just pairwise addition of p-H_2 to adsorbed cyclopropane while the latter should involve cleavage of at least one C–H bond present in the reactant molecule (see Scheme 1b for possible mechanisms). Therefore, the actual propane polarization and hence the contribution of pairwise addition routes #1–3 to the overall hydrogenation reaction may be significantly underestimated. The relative contribution of each route was not investigated in this initial report, and future mechanistic studies are certainly warranted. Moreover, future studies should certainly attempt to determine the lifetime of ^1H HP states produced via routes #2 and #3. These future studies would benefit immensely from significantly higher conversion rate (which would require massively larger catalyst quantities not available to us at the time of these experiments) and combination of PHIP with D_2 tracer studies.

In conclusion, hydrogenation of cyclopropane with p-H_2 over heterogeneous Rh/TiO_2 catalyst was shown to be a promising approach for production of HP propane with high level of proton spin polarization for MRI applications. We note that both substrate and the product of PHIP process are previously FDA-approved anesthetics, which is very advantageous for future rapid clinical translation. Relatively low chemical conversion of cyclopropane demonstrated here may be further improved by increasing the catalyst load or the use of more active catalysts. It should also be noted that significant %P_H fraction in our experiments is lost due to relaxation effects. Optimization of experimental setup may allow to reach significantly higher HP propane polarization and improved chemical conversion.[55] The formation of magnetically equivalent HP methyl protons in a pseudo singlet state likely formed via routes #2–3 is intriguing, because the produced HP states may have ultra-long life time – subject of our ongoing studies.

Experimental Section

Catalysts Preparation.

Materials: TiO_2 powder (Hombifine N, S_{BET} = 107 m^2/g), 10% palladium(II) nitrate solution in 10% nitric acid (Aldrich 380040), 8% chloroplatinic acid aqueous solution (Aldrich 262587), $RhCl_3$ hydrate (CAS 20765-98-4), NaOH (CAS 1310-73-2), HNO_3 (CAS 7697-37-2). First, $Rh(OH)_3$ and $H_2[Pt(OH)_6]$ were formed by adding an excess of alkali to $RhCl_3$ and $H_2[PtCl_6]$, respectively. The resulting precipitates were washed with excess of cold water until the negative reaction to the chloride ions, and dissolved in nitric acid. The resulting rhodium(III) and platinum(IV) nitrate solutions as well as commercial palladium(II) nitrate solutions were used for the preparation of supported Rh, Pt and Pd catalysts, respectively. The TiO_2 powder was calcinated at 500 °C for 2 h prior to use. Then TiO_2 was impregnated with the mixture of required amount of corresponding nitrate solution and water for 1 h at room temperature. The solvent excess was evaporated, and the samples were dried in air at 120 °C for 4 h and calcinated in air at 400 °C for 3 h, followed by reduction in 25/75 vol% H_2/N_2 flow at 300 °C for 3 h.

NMR and MRI Experiments.

Cyclopropane (ChemSampCo, Dallas, TX, USA, 97–99%), propene (Sigma-Aldrich, ≥99 %) and hydrogen (ultra-pure) were used as received. Hydrogen was enriched with p-H_2 either up to 50% by passing it through a copper spiral tubing with a layer of FeO(OH) powder (Sigma-Aldrich) immersed in liquid N_2 or up to 82–84% using home-built cryocooling parahydrogen generator. 50% enriched p-H_2 was used for homogeneous hydrogenation, heterogeneous liquid phase hydrogenation and some of gas phase PASADENA hydrogenation experiments (see corresponding figure captions). All other experiments were performed with 82–84% enriched p-H_2. Gas flow rates of cyclopropane and hydrogen were regulated in standard cubic centimeters per minute (sccm) using mass flow controllers (Sierra Instruments, Monterey, CA, model # C50LAL-DD-2-PV2-V0).

In PASADENA[12] experiments, hydrogenation reactions were carried out at 90 psig total pressure in medium-wall 5 mm NMR tubes (Wilmad glass P/N 503-PS-9) tightly connected with ¼ inch outer diameter (OD) PTFE tubes. For homogeneous hydrogenation experiments, the NMR tube was filled with 0.5 mL of 5 mM solution of $[Rh(NBD)(dppb)]BF_4$ (NBD = norbornadiene, dppb = 1,4-bis(diphenylphosphino)butane) in CD_3OD under Argon atmosphere and heated inside the NMR spectrometer to 40 °C. Cyclopropane and p-H_2 were bubbled through the solution either simultaneously (10 sccm cyclopropane and 30 sccm p-H_2) or sequentially (first, the solution was saturated with cyclopropane, and then p-H_2 was bubbled through at 30 sccm). For heterogeneous hydrogenation of cyclopropane in liquid phase, 10 mg of 1 wt.% Rh/TiO_2 catalyst was placed in the bottom of NMR tube and 0.5 mL of CD_3OD was added. The tube was heated inside the NMR spectrometer to 40 °C. Cyclopropane and p-H_2 were bubbled through the solution either simultaneously (15 sccm cyclopropane and 20 sccm p-H_2) or sequentially (first, the solution was saturated with cyclopropane, and then p-H_2 was bubbled through at 30 sccm). For heterogeneous gas phase hydrogenation experiments in PASADENA conditions, the catalysts (10 or 15 mg) were

placed in the bottom of the NMR tube heated to 70 or 90 °C. General scheme of PASADENA experimental setup was presented elsewhere.[48]

In ALTADENA[54] experiments, hydrogenation was carried out at 90 psig total pressure in specially designed reactor positioned outside the NMR spectrometer in Earth's magnetic field. The reactor represented a copper tubing (¼ inch OD, ~0.186-inch. inner diameter) comprised of three sections (each 16-cm length). The 1st and the 3rd sections were filled with ~13 g of 20–30 mesh copper granules, while the 2nd section was filled with the mixture of copper granules (11.4 g) and 1 wt.% Rh/TiO_2 catalyst (118 or 280 mg). Copper granules were employed to provide efficient heat exchange inside the reactor. The masses were adjusted in order to obtain ~12 cm length copper or copper+catalyst layers in all sections, which were separated by ~4 cm layers of fiberglass wool (~2 cm ends of the reactor were also filled with fiberglass). The first two sections were heated with ovens while the third one was cooled with a fan. All sections had an independent temperature control. Thus, in the 1st section gas mixture was heated to required temperature, in the 2nd one it reacted to produce HP propane, while in the 3rd one it was cooled down. The resultant gas mixture was headed to a medium-wall 5 mm NMR tube (Wilmad glass P/N 503-PS-9) located inside the NMR spectrometer. The overall scheme of ALTADENA experimental setup is presented in Figure 4.

For MRI experiments, generally the same ALTADENA setup was utilized, except that the resultant gas mixture was headed to a ~5.5 mL spherical phantom located inside a MRI scanner instead of the NMR tube. The phantom was connected with the setup using two PTFE tubing lines (mostly 1/16 inch OD, but with 1/8 inch OD connection to the phantom). Production of HP propane for MRI experiments was carried out over 280 mg of 1 wt.% Rh/TiO_2 catalyst at 140 °C, 90 psig total gas pressure and 240/480 sccm cyclopropane/H_2 gas flow rate (p-H_2 enrichment was ~82%). All NMR spectra were acquired on 9.4 T Bruker NMR spectrometer using $\pi/4$ radiofrequency (rf) pulse in PASADENA experiments and $\pi/2$ rf pulse in ALTADENA experiments. The 2D MR images were acquired on a 4.7 T Varian MRI scanner with the following imaging parameters: 2D GRE pulse sequence, 64×64 matrix with TR ~4.5 ms, no slice selection, field of view 64×64 mm^2, pixel size 1×1 mm^2.

Supplementary Material

Refer to Web version on PubMed Central for supplementary material.

Acknowledgements

OGS and KVK thank the grant from the Russian Science Foundation (17-73-20030) for the support of heterogeneous production of HP propane. IVK thanks SB RAS integrated research program (# 0333-2018-0006 / II. 1.13) and Federal Agency for Scientific Organizations #0333-2017-0002 for support of parahydrogen activation studies. EYC thanks NSF CHE-1416268 and CHE-1416432, NIH 1R21EB020323 and R21CA220137, and DOD CDMRP W81XWH-15-1-0271, and W81XWH-15-1-0272, and RFBR (17-54-33037-OHKO_a) for funding support of MRI studies. VIB and LMK thank BIC project No. 0303-2016-0004 for the support of catalysts preparation.

References

[1]. Barskiy DA, Coffey AM, Nikolaou P, Mikhaylov DM, Goodson BM, Branca RT, Lu GJ, Shapiro MG, Telkki V-V, Zhivonitko VV, Koptyug IV, Salnikov OG, Kovtunov KV, Bukhtiyarov VI, Rosen MS, Barlow MJ, Safavi S, Hall IP, Schröder L, Chekmenev EY, Chem. Eur. J 2017, 23, 725–751. [PubMed: 27711999]

[2]. Mugler JP, Altes TA, J. Magn. Reson. Imaging 2013, 37, 313–331. [PubMed: 23355432]

[3]. Nikolaou P, Goodson BM, Chekmenev EY, Chem. Eur. J 2015, 21, 3156–3166. [PubMed: 25470566]

[4]. Kuzma NN, Hakansson P, Pourfathi M, Ghosh RK, Kara H, Kadlecek SJ, Pileio G, Levitt MH, Rizi RR, J. Magn. Reson 2013, 234, 90–94. [PubMed: 23851025]

[5]. Pourfathi M, Kuzma NN, Kara H, Ghosh RK, Shaghaghi H, Kadlecek SJ, Rizi RR, J. Magn. Reson 2013, 235, 71–76. [PubMed: 23981341]

[6]. Vuichoud B, Canet E, Milani J, Bornet A, Baudouin D, Veyre L, Gajan D, Emsley L, Lesage A, Copéret C, Thieuleux C, Bodenhausen G, Koptyug I, Jannin S, J. Phys. Chem. Lett 2016, 3235–3239. [PubMed: 27483034]

[7]. Kovtunov KV, Pokochueva E, Salnikov OG, Cousin S, Kurzbach D, Vuichoud B, Jannin S, Chekmenev EY, Goodson BM, Barskiy DA, Koptyug IV, Chem. Asian J 2018, doi:10.1002/asia.201800551.

[8]. Goodson BM, J. Magn. Reson 2002, 155, 157–216. [PubMed: 12036331]

[9]. Rosen MS, Chupp TE, Coulter KP, Welsh RC, Swanson SD, Rev. Sci. Instrum 1999, 70, 1546–1552.

[10]. Goodson BM, Whiting N, Coffey AM, Nikolaou P, Shi F, Gust BM, Gemeinhardt ME, Shchepin RV, Skinner JG, Birchall JR, Barlow MJ, Chekmenev EY, Emagres 2015, 4, 797–810.

[11]. Bowers CR, Weitekamp DP, Phys. Rev. Lett 1986, 57, 2645–2648. [PubMed: 10033824]

[12]. Bowers CR, Weitekamp DP, J. Am. Chem. Soc 1987, 109, 5541–5542.

[13]. Hövener J-B, Pravdivtsev AN, Kidd B, Bowers CR, Glöggler S, Kovtunov KV, Plaumann M, Katz-Brull R, Buckenmaier K, Jerschow A, Reineri F, Theis T, Shchepin RV, Wagner S, Bhattacharya P, Zacharias NM, Chekmenev EY, Angew. Chem. Int. Ed 2018, DOI 10.1002/anie.201711842.

[14]. Eisenschmid TC, Kirss RU, Deutsch PP, Hommeltoft SI, Eisenberg R, Bargon J, Lawler RG, Balch AL, J. Am. Chem. Soc 1987, 109, 8089–8091.

[15]. Green RA, Adams RW, Duckett SB, Mewis RE, Williamson DC, Green GGR, Prog. Nucl. Mag. Res. Spectrosc 2012, 67, 1–48.

[16]. Walkup LL, Woods JC, NMR Biomed. 2014, 27, 1429–1438. [PubMed: 24953709]

[17]. Muradyan I, Butler JP, Dabaghyan M, Hrovat M, Dregely I, Ruset I, Topulos GP, Frederick E, Hatabu H, Hersman WF, Patz S, J. Magn. Reson. Imaging 2013, 37, 457–470. [PubMed: 23011916]

[18]. Lilburn DML, Pavlovskaya GE, Meersmann T, J. Magn. Reson 2013, 229, 173–186. [PubMed: 23290627]

[19]. Ouriadov A, Farag A, Kirby M, McCormack DG, Parraga G, Santyr GE, Magn. Reson. Med 2013, 70, 1699–1706. [PubMed: 23359386]

[20]. Driehuys B, Martinez-Jimenez S, Cleveland ZI, Metz GM, Beaver DM, Nouls JC, Kaushik SS, Firszt R, Willis C, Kelly KT, Wolber J, Kraft M, McAdams HP, Radiology 2012, 262, 279–289. [PubMed: 22056683]

[21]. Patz S, Hersman FW, Muradian I, Hrovat MI, Ruset IC, Ketel S, Jacobson F, Topulos GP, Hatabu H, Butler JP, Eur. J. Radiol 2007, 64, 335–344. [PubMed: 17890035]

[22]. Butler JP , Loring SH , Patz S , Tsuda A , Yablonskiy DA , Mentzer NSJ. Engl. J. Med 2012, 367, 244–247.

[23]. Albert MS, Cates GD, Driehuys B, Happer W, Saam B, Springer CS, Wishnia A, Nature 1994, 370, 199–201. [PubMed: 8028666]

[24]. Nikolaou P, Coffey AM, Walkup LL, Gust BM, Whiting NR, Newton H, Muradyan I, Dabaghyan M, Ranta K, Moroz G, Patz S, Rosen MS, Barlow MJ, Chekmenev EY, Goodson BM, Magn. Reson. Imaging 2014, 32, 541–550. [PubMed: 24631715]

[25]. Ruset IC, Ketel S, Hersman FW, Phys. Rev. Lett 2006, 96, 053002. [PubMed: 16486926]

[26]. Zook AL, Adhyaru BB, Bowers CR, J. Magn. Reson 2002, 159, 175–182. [PubMed: 12482697]

[27]. Driehuys B, Cates GD, Miron E, Sauer K, Walter DK, Happer W, Appl. Phys. Lett 1996, 69, 1668–1670.

[28]. Freeman MS, Emami K, Driehuys B, Phys. Rev. A 2014, 90, 023406. [PubMed: 25400489]

[29]. Nikolaou P, Coffey AM, Walkup LL, Gust BM, Whiting N, Newton H, Barcus S, Muradyan I, Dabaghyan M, Moroz GD, Rosen M, Patz S, Barlow MJ, Chekmenev EY, Goodson BM, Proc. Natl. Acad. Sci. U. S. A 2013, 110, 14150–14155. [PubMed: 23946420]

[30]. Nikolaou P, Coffey AM, Ranta K, Walkup LL, Gust B, Barlow MJ, Rosen MS, Goodson BM, Chekmenev EY, J. Phys. Chem. B 2014, 118, 4809–4816. [PubMed: 24731261]

[31]. Nikolaou P, Coffey AM, Walkup LL, Gust B, LaPierre C, Koehnemann E, Barlow MJ, Rosen MS, Goodson BM, Chekmenev EY, J. Am. Chem. Soc 2014, 136 1636–1642. [PubMed: 24400919]

[32]. Kovtunov KV, Barskiy DA, Coffey AM, Truong ML, Salnikov OG, Khudorozhkov AK, Inozemtseva EA, Prosvirin IP, Bukhtiyarov VI, Waddell KW, Chekmenev EY, Koptyug IV, Chem. Eur. J 2014, 20, 11636 – 11639. [PubMed: 24961814]

[33]. Bouchard LS, Kovtunov KV, Burt SR, Anwar MS, Koptyug IV, Sagdeev RZ, Pines A, Angew. Chem. Int. Ed 2007, 46, 4064–4068.

[34]. Koptyug IV, Kovtunov KV, Burt SR, Anwar MS, Hilty C, Han SI, Pines A, Sagdeev RZ, J. Am. Chem. Soc 2007, 129, 5580–5586. [PubMed: 17408268]

[35]. Bouchard LS, Burt SR, Anwar MS, Kovtunov KV, Koptyug IV, Pines A, Science 2008, 319, 442–445. [PubMed: 18218891]

[36]. Kopanski A, Hane F, Li T, Albert M, in 25th ISMRM Conference, April 22–27, Honolulu, Hawaii, 2017, p. 2162.

[37]. Duckett SB, Mewis RE, Acc. Chem. Res 2012, 45, 1247–1257. [PubMed: 22452702]

[38]. Kovtunov KV, Zhivonitko VV, Skovpin IV, Barskiy DA, Koptyug IV, Top. Curr. Chem 2013, 338, 123–180. [PubMed: 23097028]

[39]. Kovtunov KV, Truong ML, Barskiy DA, Koptyug IV, Coffey AM, Waddell KW, Chekmenev EY, Chem. Eur. J 2014, 20, 14629–14632. [PubMed: 25263795]

[40]. Kovtunov KV, Truong ML, Barskiy DA, Salnikov OG, Bukhtiyarov VI, Coffey AM, Waddell KW, Koptyug IV, Chekmenev EY, J. Phys. Chem. C 2014, 118, 28234–28243.

[41]. Corma A, Salnikov OG, Barskiy DA, Kovtunov KV, Koptyug IV, Chem. Eur. J 2015, 21, 7012–7015. [PubMed: 25754067]

[42]. Zhao EW, Maligal-Ganesh R, Xiao C, Goh T-W, Qi Z, Pei Y, Hagelin-Weaver HE, Huang W, Bowers CR, Angew. Chem. Int. Ed 2017, 56, 3925–3929.

[43]. Kovtunov KV, Romanov AS, Salnikov OG, Barskiy DA, Chekmenev EY, Koptyug IV, Tomography 2016, 2, 49–55. [PubMed: 27478870]

[44]. Barskiy DA, Salnikov OG, Romanov AS, Feldman MA, Coffey AM, Kovtunov KV, Koptyug IV, Chekmenev EY, J. Magn. Reson 2017, 276, 78–85. [PubMed: 28152435]

[45]. Burueva DB, Romanov AS, Salnikov OG, Zhivonitko VV, Chen Y-W, Barskiy DA, Chekmenev EY, Hwang DW-H, Kovtunov KV, Koptyug IV, J. Phys. Chem. C 2017, 121, 4481–4487.

[46]. McKee RH, Herron D, Saperstein M, Podhasky P, Hoffman GM, Roberts L, Int. J. Toxicol 2014, 33, 28S–51S. [PubMed: 24179026]

[47]. Boyd J, Ulster Med. J 1946, 15, 58–77.

[48]. Salnikov OG, Barskiy DA, Coffey AM, Kovtunov KV, Koptyug IV, Chekmenev EY, ChemPhysChem 2016, 17, 3395–3398. [PubMed: 27459542]

[49]. Dong Y, Ebrahimi M, Tillekaratne A, Simonovis JP, Zaera F, Phys. Chem. Chem. Phys 2016, 18, 19248–19258. [PubMed: 27373226]

[50]. Cremer PS, Su X, Shen YR, Somorjai GA, J. Phys. Chem 1996, 100, 16302–16309.

[51]. Zaera F, ACS Catalysis 2017, 7, 4947–4967.

[52]. Burueva DB, Salnikov OG, Kovtunov KV, Romanov AS, Kovtunova LM, Khudorozhkov AK, Bukhtiyarov AV, Prosvirin IP, Bukhtiyarov VI, Koptyug IV, J. Phys. Chem. C 2016, 120, 13541–13548.

[53]. Zhivonitko V, Kovtunov K, Chapovsky P, Koptyug I, Angew. Chem. Int. Ed 2013, 52, 13251–13255.

[54]. Pravica MG, Weitekamp DP, Chem. Phys. Lett 1988, 145, 255–258.

[55]. Barskiy DA, Kovtunov KV, Gerasimov EY, Phipps MA, Salnikov OG, Coffey AM, Kovtunova LM, Prosvirin IP, Bukhtiyarov VI, Koptyug IV, Chekmenev EY, J. Phys. Chem. C 2017, 121, 10038–10046.

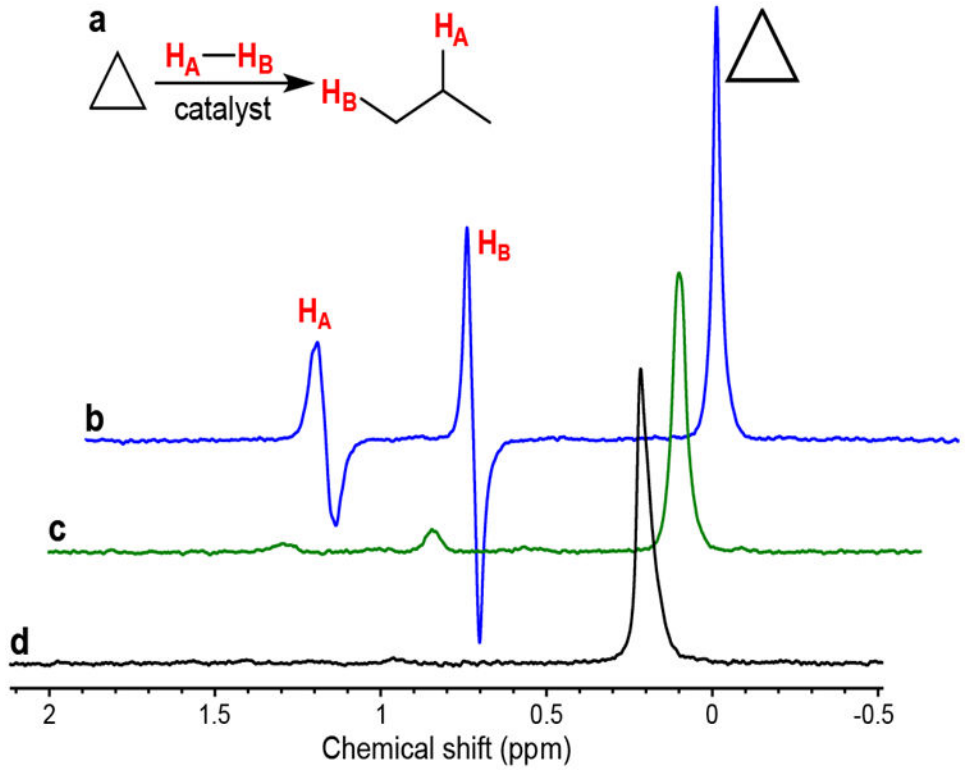

Figure 1.

(a) Reaction scheme of cyclopropane hydrogenation with p-H2. (b–d) ^{1}H NMR spectra acquired in PASADENA hydrogenation of cyclopropane with 50% enriched p-H2 at 90 °C over 10 mg of (b) 1 wt.% Rh/TiO2 catalyst, (c) 2 wt.% Pt/TiO2 catalyst, (d) 2 wt.% Pd/TiO2 catalyst in flowing gas conditions (30 sccm of cyclopropane and 100 sccm of H2 at 90 psig total pressure).

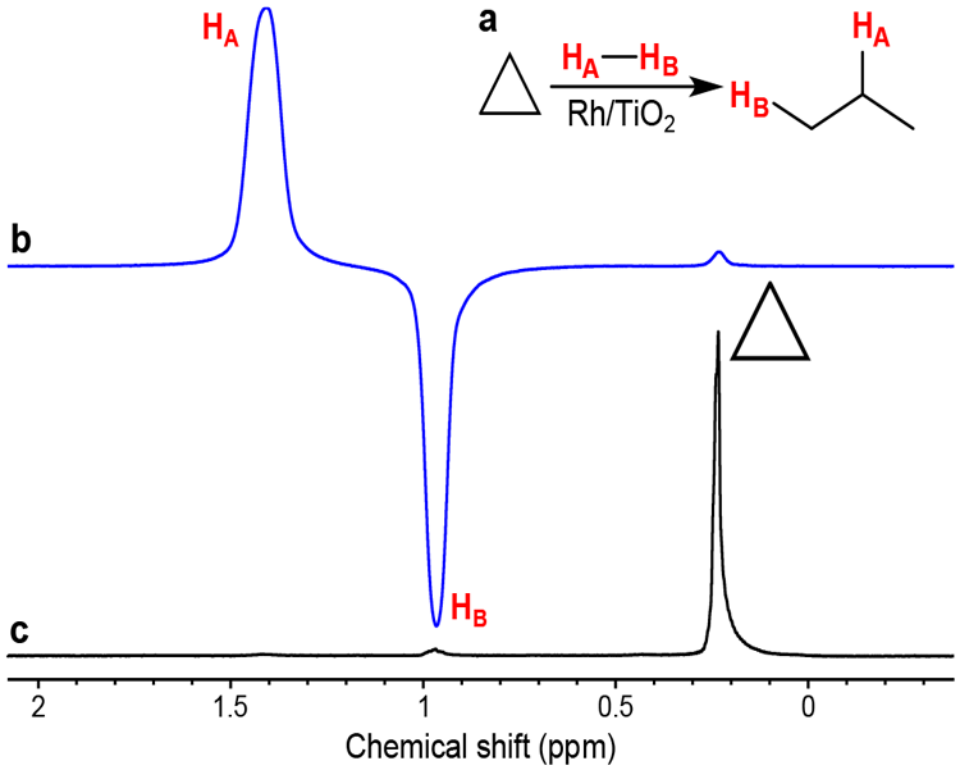

Figure 2.

(a) Reaction scheme of cyclopropane hydrogenation with p-H2 over Rh/TiO2 catalyst. (b–c) ^{1}H NMR spectra acquired in ALTADENA hydrogenation of cyclopropane with 84% enriched p-H2 at 130 °C and 90 psig total pressure over 280 mg of 1 wt.% Rh/TiO2 catalyst (b) while the gas was flowing and (c) after interruption of gas flow. The gas flow rates of cyclopropane and H2 were 240 and 480 sccm, respectively. The spectra are presented on the same vertical scale.

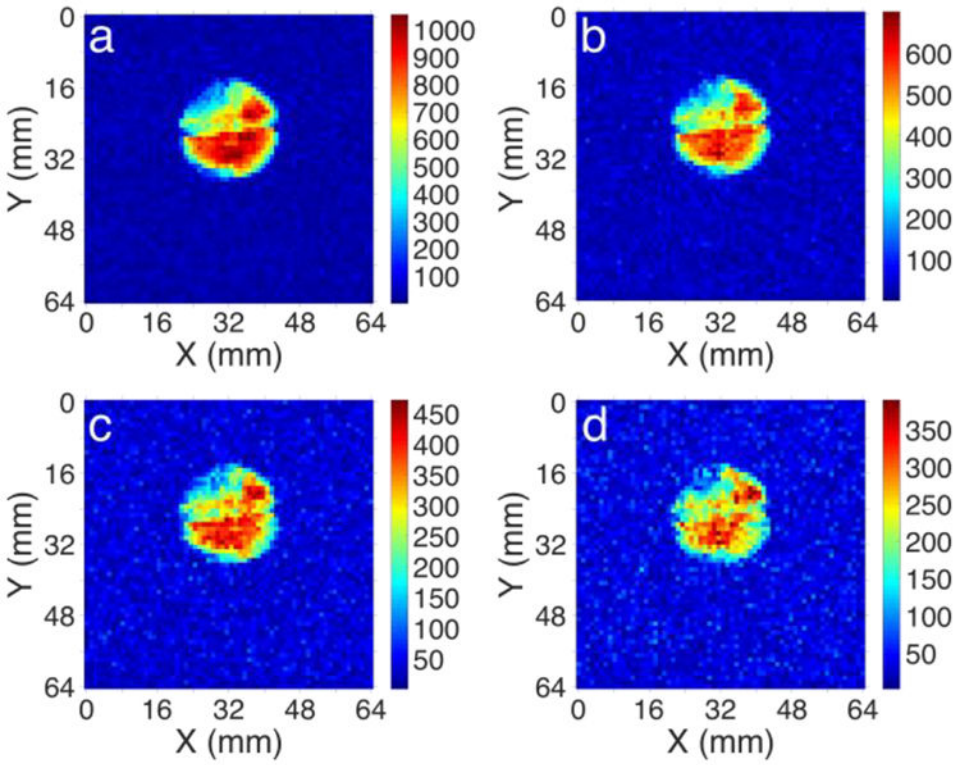

Figure 3.

2D MRI of HP propane gas in ~5.5 mL spherical phantom. HP propane was produced by hydrogenation of cyclopropane with 82% enriched p-H_2 over 280 mg of 1 wt.% Rh/TiO_2 catalyst at 140 °C and 240/480 sccm cyclopropane/H_2 gas flow rate. Images (a-d) were acquired on a 4.7 T Varian MRI scanner after interruption of gas flow every ~0.35 sec with the following imaging parameters: 2D GRE pulse sequence, 64×64 matrix with TR ~4.5 ms, no slice selection, field of view 64×64 mm^2, pixel size 1×1 mm^2. The imaging artifacts in the areas of reduced intensities are due to tubing and glue inside the phantom. The HP gas flow was stopped immediately before image acquisition. The intensity reduction in images b), c), and d) is due to T_1 relaxation of HP state.

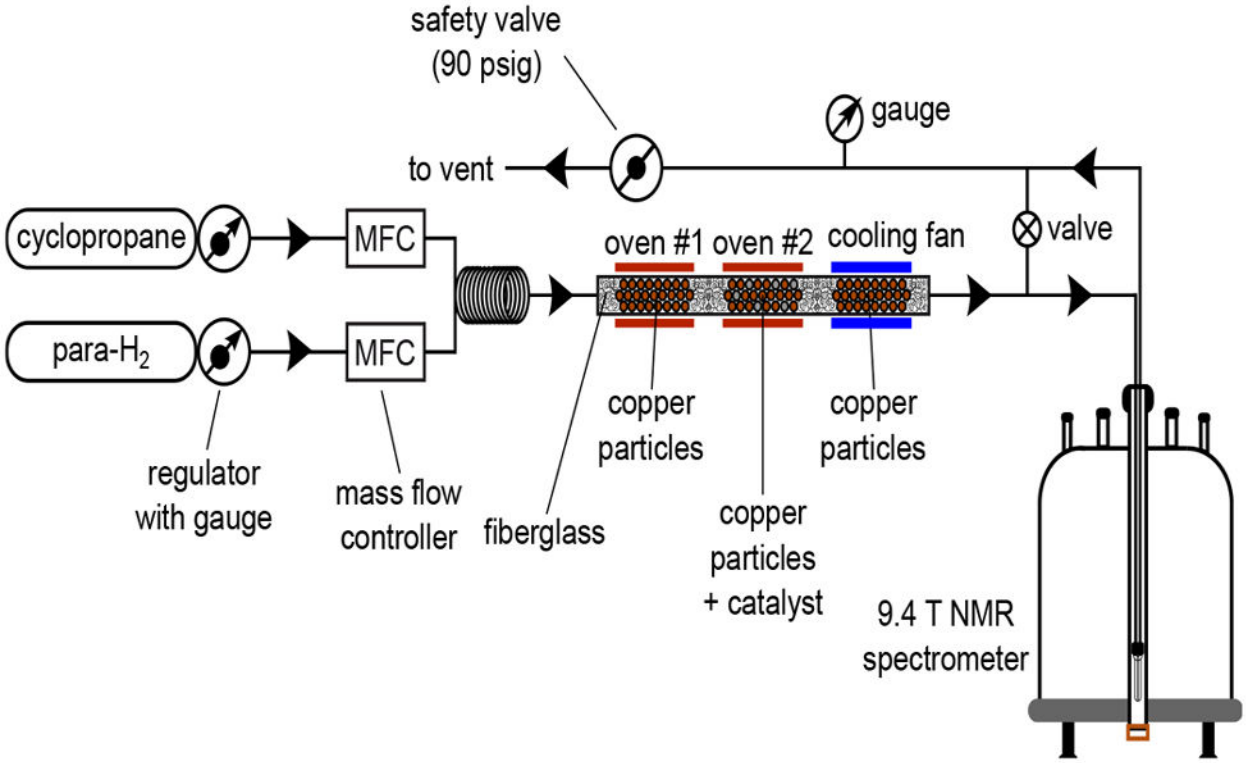

Figure 4.
Schematics of ALTADENA experimental setup.

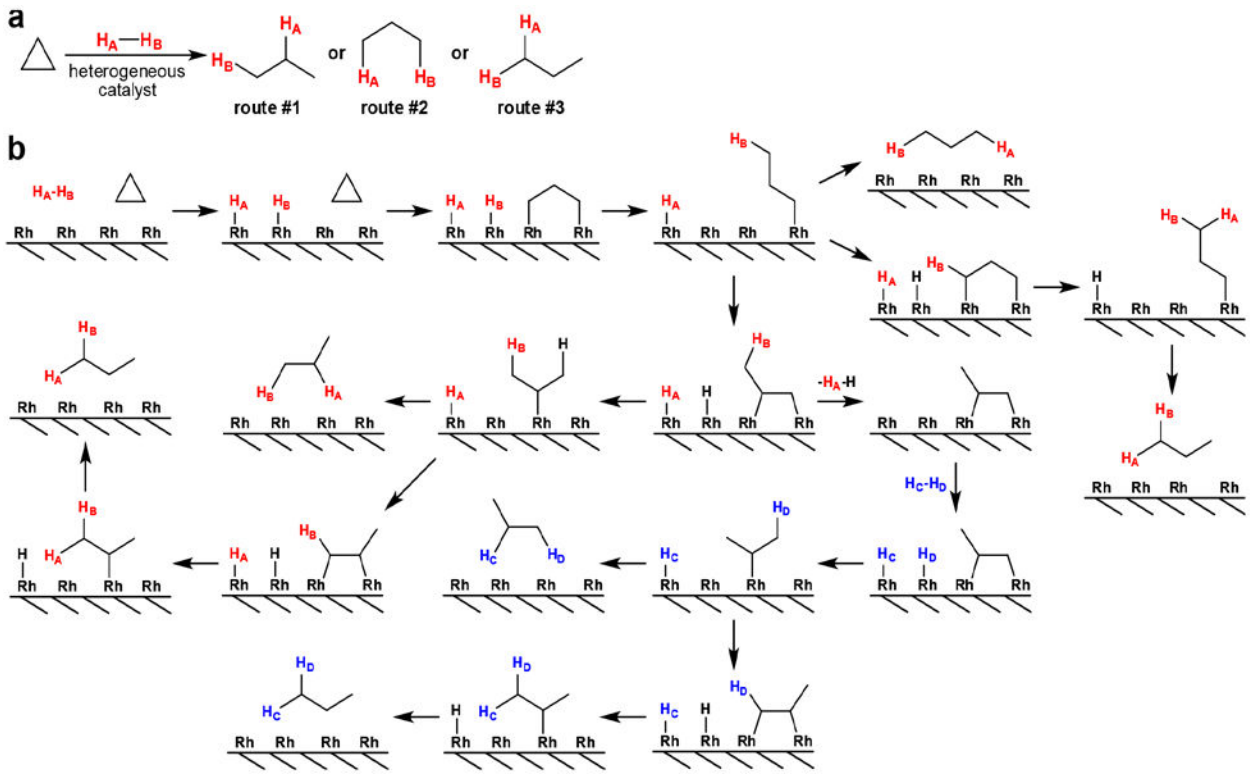

Scheme 1.

(a) Reaction scheme of cyclopropane hydrogenation with p-H_2 over heterogeneous catalyst. (b) Possible mechanisms of HP propane formation via reaction of cyclopropane with p-H_2 over Rh/TiO_2 catalyst. p-H_2 molecules are denoted as H_A-H_B and H_C-H_D.